Research Paper

Radiation of Sound from a Coaxial Duct Formed by a Semi-Infinite Rigid Outer Cylinder and Infinite Inner Cylinder Having Different Linings

Hülya ÖZTÜRK[(1)*], Burhan TIRYAKIOGLU[(2)]

[(1)] *Department of Mathematics*
Gebze Technical University
Kocaeli, Turkey
*Corresponding Author e-mail: h.ozturk@gtu.edu.tr

[(2)] *Department of Applied Mathematics*
Marmara University
Istanbul, Turkey

In the present work, the radiation of sound waves from a coaxial duct is considered. This coaxial duct has an inner wall which is infinite and has piecewise acoustically absorbent material, while the outer wall is semi-infinite and rigid. The analytical solution of the problem is found by means of the Wiener-Hopf technique. Applying the Fourier transformation to the boundary value problem, the explicit expression for the scattered field is obtained. In the end, some numerical results are displayed for different parameters and compared to rigid case.

Keywords: Wiener-Hopf technique; absorbent lining; coaxial duct; acoustic radiation.

1. Introduction

The investigation of sound wave propagation and radiation is an important subject in noise pollution and relevant for many engineering applications. For this reason, lots of semi-infinite or infinite cylindrical structures which include the aperture or acoustically absorbent lining on their inner or outer walls have been investigated by numerous authors. Analytical solution for the problem of sound radiation from a semi-infinite unflanged rigid circular duct has been obtained by LEVINE and SCHWINGER (1948) via Wiener-Hopf method. Wiener-Hopf technique has been used in acoustic problems extensively (LAWRIE *et al.*, 1993; BUYUKAKSOY, POLAT, 1998; ÇINAR, 2013; SNAKOWSKA *et al.*, 2017; OZTURK, 2020). Case in which the inner wall of an infinite annular duct has a finite aperture has been considered by ÇINAR *et al.* (2011). Also, as a very effective parameter, absorbing lining first has been theoretically studied in the literature (MORSE, 1939; CREMER, 1953; LAPIN, 1975). The common ground of these studies is that they examine an infinite ducts. RAWLINS (1978) later has revealed the effect of internal duct lining on the radia-

tion from semi-infinite rigid duct. Besides, DEMIR and BUYUKAKSOY (2003) have investigated the rigid circular cylindrical pipe with a partial internal impedance loading. Recently, the acoustic radiation by a semi-infinite duct with outer lining and perforated end is analyzed rigorously by TIRYAKIOGLU (2020). In addition to all these studies, the absorbing lining has been investigated extensively with and without flow in the literature (REINSTRA, 2007; TIWANA *et al.*, 2017; PEAKE, ABRAHAMS, 2020).

From these investigations we concluded that it is neccessary to adopt different geometries and parameters to reduce noise pollution. For this purpose, a coaxial duct with a semi-infinite rigid outer cylinder and an infinite inner cylinder having different linings has been considered. In order to provide noise reduction, such structures have been used as a model for many engineering applications, such as exhausts of automobile engines, modern aircraft jet and turbofan engines, etc. By using the Fourier transform technique in conjunction with the Wiener-Hopf method, a rigorous solution of the related boundary value problem is obtained. It is shown that the presence of different inner duct linings makes significance loss on sound pressure levels

when it is compared with the rigid duct. The effect of these parameters is presented graphically in Sec. 7 in detail. Throughout this paper a time dependence $e^{-i\omega t}$ is assumed, where ω is the angular frequency.

2. Formulation of the problem

We shall consider the acoustic radiation of the wave mode from a coaxial duct with a semi infinite rigid outer duct and an infinite two-part acoustic impedance inner duct. From the symmetry of the geometry of the problem and of the incident field, the total field will be independent of azimuth ϕ everywhere in circular cylindrical coordinate system (ρ, ϕ, z). Therefore, a scalar potential $\psi(\rho, z)$ which defines the acoustic pressure and velocity by $p = i\omega\rho_0\psi$ and $\mathbf{v} = \text{grad}\,\psi$, respectively, is introduced. Here ρ_0 is the density of the undisturbed medium. The liner impedances are denoted by $Z_1(z \in (-\infty, 0))$ and $Z_2(z \in (0, \infty))$, respectively. In Fig. 1, $\eta_{1,2} = \rho_0 c/Z_{1,2}$ are the specific admittances where c is the velocity of sound. Duct walls are assumed to be infinitely thin. The outer duct occupies the region $\{\rho = b, -\infty < z < 0\}$ while the inner duct occupies the region $\{\rho = a, -\infty < z < \infty\}$ as shown in Fig. 1.
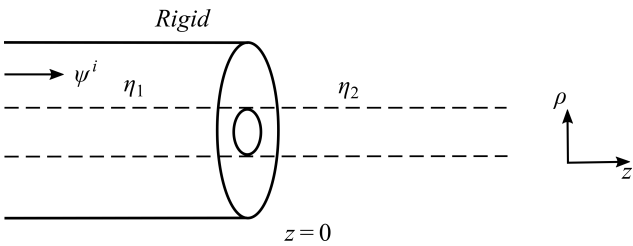

Fig. 1. Geometry of the problem.

Let the incident sound field is taken to be

$$\psi^i(\rho, z) = [ik\eta_1 S(a, \rho, \sigma_n) - S'(\rho, a, \sigma_n)]e^{i\varkappa_n z}, \quad (1)_1$$

where

$$S(a, \rho, \sigma_n) = [Y_0(\sigma_n a)J_0(\sigma_n\rho) - J_0(\sigma_n a)Y_0(\sigma_n\rho)]. \quad (1)_2$$

Above, derivative with respect to ρ is denoted by a prime $(')$ and $\varkappa_n$ is the root of the equation

$$ik\eta_1[Y_1(\sigma_n b)J_0(\sigma_n a) - J_1(\sigma_n b)Y_0(\sigma_n a)]$$
$$+\sigma_n ik\eta_1[Y_1(\sigma_n a)J_1(\sigma_n b) - J_1(\sigma_n a)Y_1(\sigma_n b)] = 0 \quad (1)_3$$

with

$$\varkappa_n = \sqrt{k^2 - \sigma_n^2}. \quad (1)_4$$

Here J_n and Y_n $(n = 0, 1)$ are the well-known Bessel and Neumann functions, $k = \omega/c$ denotes the wave number of the medium. In order to obtain the solution, the total diffracted field can be defined as

$$\psi^T(\rho, z) = \begin{cases} \psi_1(\rho, z); & \rho > b, \\ \psi_2(\rho, z) + \psi^i(\rho, z); & a < \rho < b, \end{cases} \quad (2)$$

where $\psi_j(\rho, z)$, $j = 1, 2$ are the potential functions which satisfy the following Helmholtz equation

$$\left[\frac{1}{\rho}\frac{\partial}{\partial\rho}\left(\rho\frac{\partial}{\partial\rho}\right) + \frac{\partial^2}{\partial z^2} + k^2\right]\psi_j(\rho, z) = 0, \quad j = 1, 2 \quad (3)$$

and the following conditions:

$$\frac{\partial}{\partial\rho}\psi_1(b, z) = 0, \quad z < 0,$$

$$\frac{\partial}{\partial\rho}\psi_2(b, z) = 0, \quad z < 0,$$

$$\left(ik\eta_1 + \frac{\partial}{\partial\rho}\right)\psi_2(a, z) = 0, \quad z < 0,$$

$$\psi_1(b, z) = \psi_2(b, z) + \psi^i(b, z), \quad z > 0, \quad (4)$$

$$\left(ik\eta_2 + \frac{\partial}{\partial\rho}\right)[\psi_2(a, z) + \psi^i(a, z)] = 0, \quad z > 0,$$

$$\frac{\partial}{\partial\rho}\psi_1(b, z) = \frac{\partial}{\partial\rho}\psi_2(b, z), \quad z > 0.$$

3. Derivation of the Wiener-Hopf equation

The unknown fields $\psi_1(\rho, z)$ and $\psi_2(\rho, z)$ satisfy (3) for $z \in (-\infty, \infty)$. By taking Fourier transform of these equations, one can obtain the following integral representations

$$\psi_1(\rho, z) = \int_L A(\alpha)H_0^{(1)}(K\rho)e^{-i\alpha z}\,\mathrm{d}\alpha,$$

$$\psi_2(\rho, z) = \int_L [B(\alpha)J_0(K\rho) + C(\alpha)Y_0(K\rho)]e^{-i\alpha z}\,\mathrm{d}\alpha, \quad (5)$$

where L is an inverse Fourier transform integration contour in the complex α-plane. $A(\alpha)$, $B(\alpha)$, and $C(\alpha)$ are spectral coefficients to be determined. $H_0^{(1)} = J_0 + iY_0$ is the Hankel function of the first type. $K = \sqrt{k^2 - \alpha^2}$ is the square root function which is defined in the complex α-plane (RIENSTRA, PEAKE, 2005). Applying the boundary condition $(4)_1$ and $(4)_3$ on $\rho = b$, $\rho = a$ respectively and taking Fourier transforms give

$$-A(\alpha)KH_1^{(1)}(Kb) = \Phi_1^+(\alpha), \quad (6)$$

$$B(\alpha)J(\eta_1, \alpha) + C(\alpha)Y(\eta_1, \alpha) = \Phi_2^+(\alpha). \quad (7)$$

Similarly, continuity relations for $(4)_4$ and $(4)_5$ at $\rho = b$, $\rho = a$ give

$$A(\alpha)H_0^{(1)}(Kb) - B(\alpha)J_0(Kb) - C(\alpha)Y_0(Kb)$$
$$+\frac{F(b, \sigma_n)}{2\pi i(\varkappa_0 + \alpha)} = \Phi_1^-(\alpha), \quad (8)$$

$$B(\alpha)J(\eta_2, \alpha) + C(\alpha)Y(\eta_2, \alpha) = \Phi_2^-(\alpha)$$
$$+\frac{1}{2\pi i(\varkappa_0 + \alpha)}[ik\eta_2 F(a, \sigma_n) + F'(a, \sigma_n)], \quad (9)$$

where

$$J(\eta_m, \alpha) = ik\eta_m J_0(Ka) - KJ_1(Ka), \quad m = 1, 2,$$

$$Y(\eta_m, \alpha) = ik\eta_m Y_0(Ka) - KY_1(Ka), \quad m = 1, 2, \quad (10)$$

$$F(\rho, \sigma_n) = ik\eta_1 S(a, \rho, \sigma_n) - S'(\rho, a, \sigma_n).$$

By using $(4)_1$, $(4)_2$ together with $(4)_6$ and taking Fourier transform gives

$$A(\alpha)H_1^{(1)}(Kb) = B(\alpha)J_1(Kb) + C(\alpha)Y_1(Kb), \quad (11)$$

where $\Phi_{1,2}^+(\alpha)$ and $\Phi_{1,2}^-(\alpha)$ are analytic functions in the upper $(\operatorname{Im}\alpha > \operatorname{Im}(-k))$ and in the lower $(\operatorname{Im}\alpha < \operatorname{Im}k)$ half planes, respectively and defined as

$$\Phi_1^+(\alpha) = \frac{1}{2\pi}\int_0^\infty \frac{\partial}{\partial\rho}\psi_1(b, z)e^{i\alpha z}\,\mathrm{d}z,$$

$$\Phi_2^+(\alpha) = \frac{1}{2\pi}\int_0^\infty \left(ik\eta_1 + \frac{\partial}{\partial\rho}\right)\psi_2(a, z)e^{i\alpha z}\,\mathrm{d}z,$$

$$\tag{12}$$

$$\Phi_1^-(\alpha) = \frac{1}{2\pi}\int_{-\infty}^0 \left[\psi_1(b, z) - \psi_2(b, z)\right]e^{i\alpha z}\,\mathrm{d}z,$$

$$\Phi_2^-(\alpha) = \frac{1}{2\pi}\int_{-\infty}^0 \left(ik\eta_2 + \frac{\partial}{\partial\rho}\right)\psi_2(a, z)e^{i\alpha z}\,\mathrm{d}z.$$

From the relations (6) and (11), we obtain

$$B(\alpha)KJ_1(Kb) + C(\alpha)KY_1(Kb) = -\Phi_1^+(\alpha), \quad (13)$$

$Y_1(Kb)$ and $J_1(Kb)$ can be eliminated from Eqs (11) and (13), one gets

$$B(\alpha) = \frac{1}{K}\frac{Y(\eta_1, \alpha)\Phi_1^+(\alpha) + KY_1(Kb)\Phi_2^+(\alpha)}{Y_1(Kb)J(\eta_1, \alpha) - J_1(Kb)Y(\eta_1, \alpha)},$$

$$\tag{14}$$

$$C(\alpha) = -\frac{1}{K}\frac{J(\eta_1, \alpha)\Phi_1^+(\alpha) + KJ_1(Kb)\Phi_2^+(\alpha)}{Y_1(Kb)J(\eta_1, \alpha) - J_1(Kb)Y(\eta_1, \alpha)}.$$

The substitution of $A(\alpha)$, $B(\alpha)$, and $C(\alpha)$ given by Eqs (6) and (14) into Eqs (8), (9) yields

$$\left[a^* - \frac{H_0^{(1)}(Kb)}{KH_1^{(1)}(Kb)}\right]\Phi_1^+(\alpha)$$

$$+ \frac{2}{\pi Kb}\frac{\Phi_2^+(\alpha)}{Y_1(Kb)J(\eta_1, \alpha) - J_1(Kb)Y(\eta_1, \alpha)}$$

$$+ \frac{F(b, \sigma_n)}{2\pi i(\varkappa_0 + \alpha)} = \Phi_1^-(\alpha),$$

$$\tag{15}$$

$$\frac{2ik}{\pi a}\frac{(\eta_2 - \eta_1)\Phi_1^+(\alpha)}{K\left[Y_1(Kb)J(\eta_1, \alpha) - J_1(Kb)Y(\eta_1, \alpha)\right]}$$

$$+ \frac{Y_1(Kb)J(\eta_2, \alpha) - J_1(Kb)Y(\eta_2, \alpha)}{Y_1(Kb)J(\eta_1, \alpha) - J_1(Kb)Y(\eta_1, \alpha)}\Phi_2^+(\alpha)$$

$$= \Phi_2^-(\alpha) + \frac{\left[ik\eta_2 F(a, \sigma_n) + F'(a, \sigma_n)\right]}{2\pi i(\varkappa_0 + \alpha)},$$

where

$$a^* = \frac{J(\eta_1, \alpha)Y_0(Kb) - Y(\eta_1, \alpha)J_0(Kb)}{K\left[Y_1(Kb)J(\eta_1, \alpha) - J_1(Kb)Y(\eta_1, \alpha)\right]}.$$

$\Phi_2^+(\alpha)$ can be eliminated from Eqs $(15)_1$ and $(15)_2$, then we get the following two systems of Wiener-Hopf equation:

$$M_1(\alpha)\Phi_2^-(\alpha) + \frac{M_1(\alpha)\left[ik\eta_2 F(a, \sigma_n) + F'(a, \sigma_n)\right]}{2\pi i(\varkappa_0 + \alpha)}$$

$$= \frac{2ik(\eta_2 - \eta_1)\Phi_1^+(\alpha)}{\pi aK\left[Y_1(Kb)J(\eta_2, \alpha) - J_1(Kb)Y(\eta_2, \alpha)\right]} + \Phi_2^+(\alpha),$$

$$M_2(\alpha)\Phi_1^+(\alpha) = \frac{b^*\Phi_2^-(\alpha)}{\left[Y_1(Kb)J(\eta_2, \alpha) - J_1(Kb)Y(\eta_2, \alpha)\right]}$$

$$+ \frac{b^*\left[ik\eta_2 F(a, \sigma_n) + F'(a, \sigma_n)\right]}{\left[Y_1(Kb)J(\eta_2, \alpha) - J_1(Kb)Y(\eta_2, \alpha)\right]2\pi i(\varkappa_0 + \alpha)}$$

$$- \Phi_1^-(\alpha) + \frac{F(b, \sigma_n)}{2\pi i(\varkappa_0 + \alpha)},$$

$$\tag{16}$$

where

$$b^* = J_1(Kb)Y_0(Kb) - Y_1(Kb)J_0(Kb),$$

and $M_1(\alpha)$ and $M_2(\alpha)$ are kernel functions to be factorized

$$M_1(\alpha) = \frac{Y_1(Kb)J(\eta_1, \alpha) - J_1(Kb)Y(\eta_1, \alpha)}{Y_1(Kb)J(\eta_2, \alpha) - J_1(Kb)Y(\eta_2, \alpha)},$$

$$\tag{17}$$

$$M_2(\alpha) = -\frac{2\left[J(\eta_2, \alpha) + iY(\eta_2, \alpha)\right]}{c^*KH_1^{(1)}(Kb)},$$

where

$$c^* = \pi Kb[Y_1(Kb)J(\eta_2, \alpha) - J_1(Kb)Y(\eta_2, \alpha)].$$

4. Solution of the Wiener-Hopf Equation

Consider first the Wiener-Hopf equation in $(16)_1$ and rearrange it using $(17)_1$ in the following form

$$\frac{\Phi_2^-(\alpha)}{M_1^-(\alpha)} + \frac{\left[ik\eta_2 F(a, \sigma_n) + F'(a, \sigma_n)\right]}{2\pi i(\varkappa_0 + \alpha)M_1^-(\alpha)}$$

$$= \frac{2ik(\eta_2 - \eta_1)}{\pi aK\left[Y_1(Kb)J(\eta_2, \alpha) - J_1(Kb)Y(\eta_2, \alpha)\right]}\frac{\Phi_1^+(\alpha)}{M_1^+(\alpha)}$$

$$+ \frac{\Phi_2^+(\alpha)}{M_1^+(\alpha)}.$$

$$\tag{18}$$

Here, $M_1^+(\alpha)$ and $M_1^-(\alpha)$ are the split functions, regular and free of zeros in the upper and lower half planes, respectively, result from the factorization of $M_1(\alpha)$ as,

$$M_1(\alpha) = \frac{M_1^+(\alpha)}{M_1^-(\alpha)}.$$

$$\tag{19}$$

The right hand side of Eq. (18) is analytic in the upper half plane except for the poles of the first term resulting from the zeros of

$$K\left[Y_1(Kb)J(\eta_2,\alpha) - J_1(Kb)Y(\eta_2,\alpha)\right]$$

lying in the upper half-plane, namely at $\alpha = \alpha_m$ with

$$\sqrt{k^2 - \alpha_m^2}\left[Y_1\left(\sqrt{k^2 - \alpha_m^2}\,b\right)J(\eta_2,\alpha_m)\right.$$
$$\left. - J_1\left(\sqrt{k^2 - \alpha_m^2}\,b\right)Y(\eta_2,\alpha_m)\right] = 0. \quad (20)$$

If the infinite system of poles are substracted from both sides of Eq. (18), we obtain

$$\frac{\Phi_2^-(\alpha)}{M_1^-(\alpha)} - \sum_{m=1}^{\infty}\frac{f_m}{(\alpha - \alpha_m)}$$

$$+ \frac{ik\eta_2 F(a,\sigma_n) + F'(a,\sigma_n)}{2\pi i(\varkappa_0 + \alpha)}\left[\frac{1}{M_1^-(\alpha)} - \frac{1}{M_1^-(-\varkappa_0)}\right]$$

$$= -\frac{ik\eta_2 F(a,\sigma_n) + F'(a,\sigma_n)}{2\pi i(\varkappa_0 + \alpha)M_1^-(-\varkappa_0)} - \sum_{m=1}^{\infty}\frac{f_m}{(\alpha - \alpha_m)} + \frac{\Phi_2^+(\alpha)}{M_1^+(\alpha)}$$

$$+ \frac{2ik(\eta_2 - \eta_1)}{\pi a K\left[Y_1(Kb)J(\eta_2,\alpha) - J_1(Kb)Y(\eta_2,\alpha)\right]}\frac{\Phi_1^+(\alpha)}{M_1^+(\alpha)}, \quad (21)$$

where

$$f_m = \frac{2ik(\eta_2 - \eta_1)\Phi_1^+(\alpha_m)}{\pi a M_1^+(\alpha_m)}$$

$$\cdot \lim_{\alpha \to \alpha_m}\frac{1}{\frac{d}{d\alpha}K\left[Y_1(Kb)J(\eta_2,\alpha) - J_1(Kb)Y(\eta_2,\alpha)\right]}. \quad (22)$$

The application of the analytical continuation principle together with the Liouville's theorem yields

$$\Phi_2^-(\alpha) = M_1^-(\alpha)\sum_{m=1}^{\infty}\frac{f_m}{(\alpha - \alpha_m)}$$

$$- \frac{\left[ik\eta_2 F(a,\sigma_n) + F'(a,\sigma_n)\right]M_1^-(\alpha)}{2\pi i(\varkappa_0 + \alpha)}$$

$$\cdot\left(\frac{1}{M_1^-(\alpha)} - \frac{1}{M_1^-(-\varkappa_0)}\right). \quad (23)$$

Next we consider Eq. (16)$_2$. By using the classical factorization and decomposition procedure, we get

$$M_2^+(\alpha)\Phi_1^+(\alpha) = \frac{2M_2^-(\alpha)\Phi_2^-(\alpha)}{\pi Kb\left[Y_1(Kb)J(\eta_2,\alpha) - J_1(Kb)Y(\eta_2,\alpha)\right]}$$

$$+ \frac{\left[ik\eta_2 F(a,\sigma_n) + F'(a,\sigma_n)\right]M_2^-(\alpha)}{\pi Kb\left[Y_1(Kb)J(\eta_2,\alpha) - J_1(Kb)Y(\eta_2,\alpha)\right]\pi i(\varkappa_0 + \alpha)}$$

$$- M_2^-(\alpha)\Phi_1^-(\alpha) + \frac{F(b,\sigma_n)M_2^-(\alpha)}{2\pi i(\varkappa_0 + \alpha)}, \quad (24)$$

where the split functions $M_2^+(\alpha)$ and $M_2^-(\alpha)$, result from the factorization of $M_2(\alpha)$ as,

$$M_2(\alpha) = \frac{M_2^+(\alpha)}{M_2^-(\alpha)}, \quad (25)$$

they are regular and free of zeros in the upper and lower half planes, respectively. The regularity of the right hand side of (24) is violated by the zeros on the lower half plane. Subtraction of the residue contribution of these poles as an infinite sum from both sides and using Liouville's theorem, we get the Wiener-Hopf solution

$$\Phi_1^+(\alpha) = \frac{1}{M_2^+(\alpha)}\left[\frac{F(b,\sigma_n)M_2^-(-\varkappa_0)}{2\pi i(\varkappa_0 + \alpha)}\right.$$

$$\left. + \sum_{m=1}^{\infty}\frac{g_m}{(\alpha + \alpha_m)} + \sum_{m=1}^{\infty}\frac{r_m}{(\alpha + \alpha_m)}\right]$$

$$+ \frac{\left[ik\eta_2 F(\xi_0,a) + F'(\xi_0,a)\right]M_2^-(-\varkappa_0)}{\pi b\pi i(\varkappa_0 + \alpha)M_2^+(\alpha)}$$

$$\cdot \lim_{\alpha \to -\varkappa_0}\frac{1}{K\left[Y_1(Kb)J(\eta_2,\alpha) - J_1(Kb)Y(\eta_2,\alpha)\right]}, \quad (26)$$

where

$$g_m = \frac{2M_2^-(-\alpha_m)\Phi_2^-(-\alpha_m)}{\pi b}$$

$$\cdot \lim_{\alpha \to \alpha_m}\frac{1}{\frac{d}{d\alpha}K\left[Y_1(Kb)J(\eta_2,\alpha) - J_1(Kb)Y(\eta_2,\alpha)\right]}, \quad (27)$$

$$r_m = \frac{\left[ik\eta_2 F(a,\sigma_n) + F'(a,\sigma_n)\right]M_2^-(-\alpha_m)}{\pi b\pi i(\varkappa_0 - \alpha_m)}$$

$$\cdot \lim_{\alpha \to \alpha_m}\frac{1}{\frac{d}{d\alpha}K\left[Y_1(Kb)J(\eta_2,\alpha) - J_1(Kb)Y(\eta_2,\alpha)\right]}. \quad (28)$$

5. Determining the coefficient f_m and g_m

Wiener-Hopf solutions (23) and (26) contain unknown coefficients f_m and g_m which have to be determined. Substituting $\alpha = -\alpha_r$ in Eq. (23) and using the relation in (27) we obtain

$$\frac{\pi b}{2}\frac{\lim_{\alpha \to -\alpha_r}\frac{d}{d\alpha}K\left[Y_1(Kb)J(\eta_2,\alpha) - J_1(Kb)Y(\eta_2,\alpha)\right]}{M_2^-(-\alpha_r)}g_r$$

$$= M_1^-(-\alpha_r)\sum_{m=1}^{\infty}\frac{f_m}{(-\alpha_r - \alpha_m)}$$

$$- \frac{M_1^-(-\alpha_r)\left[ik\eta_2 F(a,\sigma_n) + F'(a,\sigma_n)\right]}{2\pi i(\varkappa_0 - \alpha_r)}$$

$$\cdot\left(\frac{1}{M_1^-(-\alpha_r)} - \frac{1}{M_1^-(-\varkappa_0)}\right). \quad (29)$$

Similarly substituting $\alpha = \alpha_r$ in Eq. (26) and using the relation in (22) we obtain

$$
\frac{\pi a M_1^+(\alpha_r)}{2ik(\eta_2 - \eta_1)} \lim_{\alpha \to \alpha_r} \frac{d}{d\alpha}
$$

$$
\cdot K \left[Y_1(Kb) J(\eta_2, \alpha) - J_1(Kb) Y(\eta_2, \alpha) \right] f_r
$$

$$
= \frac{F(b, \sigma_n) M_2^-(-\varkappa_0)}{2\pi i(\varkappa_0 + \alpha_r) M_2^+(\alpha_r)} + \frac{1}{M_2^+(\alpha_r)} \sum_{m=1}^{\infty} \frac{g_m}{\alpha_r + \alpha_m}
$$

$$
+ \sum_{m=1}^{\infty} \frac{r_m}{(\alpha_r + \alpha_m) M_2^+(\alpha_r)}
$$

$$
+ \frac{\left[ik\eta_2 F(\xi_0, a) + F'(\xi_0, a) \right] M_2^-(-\varkappa_0)}{\pi b \pi i(\varkappa_0 + \alpha_r) M_2^+(\alpha_r)}
$$

$$
\cdot \lim_{\alpha \to -\varkappa_0} \frac{1}{K \left[Y_1(Kb) J(\eta_2, \alpha) - J_1(Kb) Y(\eta_2, \alpha) \right]}. \quad (30)
$$

To determine unknown coefficients f_m and g_m these systems of algebraic equations will be solved numerically.

6. Far field

The radiated field in the region $\rho > b$ can be evaluated from $(5)_1$ and using (6)

$$
\psi_1(\rho, z) = - \int_L \frac{\Phi_1^+(\alpha)}{K H_1^{(1)}(Kb)} H_0^{(1)}(K\rho) e^{-i\alpha z} \, d\alpha. \quad (31)
$$

Utilizing the asymptotic expansion of $H_0^{(1)}(K\rho)$ as $k\rho \to \infty$

$$
H_0^{(1)}(K\rho) = \sqrt{\frac{2}{\pi K \rho}} e^{iK\rho - i\pi/4}. \quad (32)
$$

The substitution $\alpha = -k \cos \mu$ in Eq. (31) and making the following substitutions

$$
\rho = r \sin \theta, \qquad z = r \cos \theta, \quad (33)
$$

the integral can be evaluated through the saddle-point technique (SNAKOWSKA, IDCZAK, 2006), we obtain

$$
\psi_1(r, \theta) \sim 2i \frac{\Phi_1^+(-k \cos \theta)}{\sin \theta H_1^{(1)}(kb \sin \theta)} \frac{e^{ikr}}{kr}. \quad (34)
$$

Here r and θ are the usual spherical coordinates.

7. Results

In this section, some computational results displaying the effect of various parameters such as the surface impedances, the radii of the inner and outer ducts and the frequency on the sound pressure level are

presented. In these figures, the Sound Pressure Level (SPL) is defined as

$$
\text{SPL} = 20 \log_{10} \left| \frac{p}{2 \cdot 10^{-5}} \right|,
$$

where p is the amplitude of the acoustic pressure of the sound wave, with the observation angle θ changing from 0 to π. The far field values are plotted at a distance 46 m away from the duct edge (DEMIR, RIENSTRA, 2010). The problem parameters related to absorbing lining are chosen from the studies of (TIRYAKIOGLU, 2019; PEAKE, ABRAHAMS, 2020) which are exist in the literature. During the numerical analysis, since the series converge rapidly the infinite set of linear algebraic equations is solved by truncating the infinite series at some number N. It can be seen from Fig. 2 that the sound pressure level becomes insensitive to the truncation number N for $N > 2$ with different values of observation angle. Hence for the numerical examples, the truncation number N is chosen by taking into account this criterion.
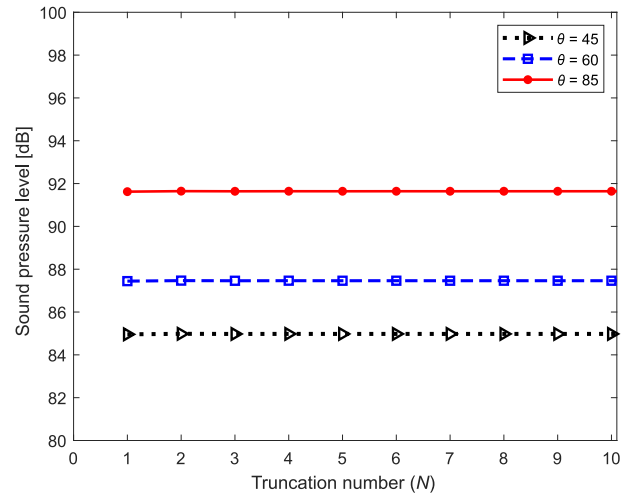
Fig. 2. Sound pressure level *versus* the truncation number N with $f = 1000$ Hz, $a = 0.025$ m, $b = 0.050$ m, $\eta_1^{-1} = 1 - i$, $\eta_2^{-1} = 2 - i$.

In order to show the effectiveness of the lining, the sound pressure level is computed numerically for some particular values and compared to rigid case in Figs 3
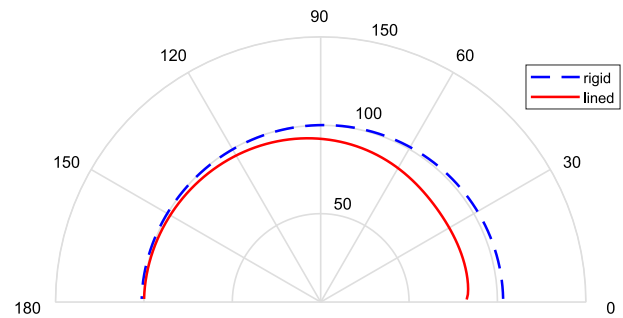
Fig. 3. Sound pressure level for rigid-lined duct with $f = 1000$ Hz, $a = 0.025$ m, $b = 0.050$ m, $\eta_1^{-1} = 1 - i$, $\eta_2^{-1} = 2 - i$.

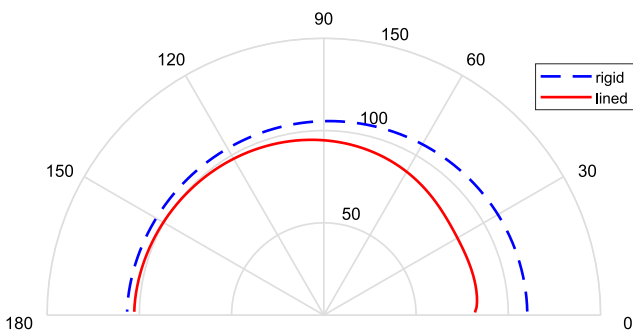and 4. It is observed that existing of lining makes significant decrease in the sound pressure level.

Fig. 4. Sound pressure level for rigid-lined duct with $f = 1500$ Hz, $a = 0.025$ m, $b = 0.050$ m, $\eta_1^{-1} = 1 - i$, $\eta_2^{-1} = 2 - i$.

Figures 5 and 6 show how the acoustically absorbent material affects the sound pressure level. Note that the sound pressure level can be reduced by changing the values of real and imaginary part of the liner impedance.
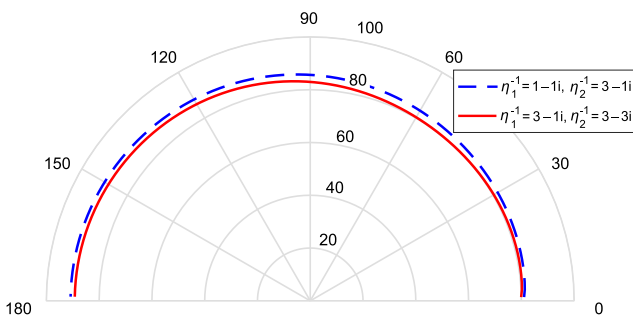

Fig. 5. Sound pressure level for different values of impedances with $f = 1000$ Hz, $a = 0.015$ m, $b = 1.5a$.
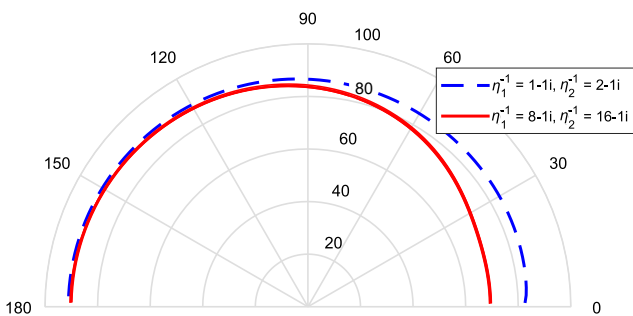
Fig. 6. Sound pressure level for different values of impedances with $f = 1000$ Hz, $a = 0.015$ m, $b = 1.5a$.

Figures 7, 8, and 9 depict the sound pressure level versus the observation angle for different values of a, b, and f. Again it is observed that these different parameter values can be used to decrease the sound pressure level.

Figures 10 and 11 depict the variation of the sound pressure level versus the imaginary part of the impedances for different values of the real part of the impedances while $a = 0.015$ m, $b = 1.5a$, $f =$
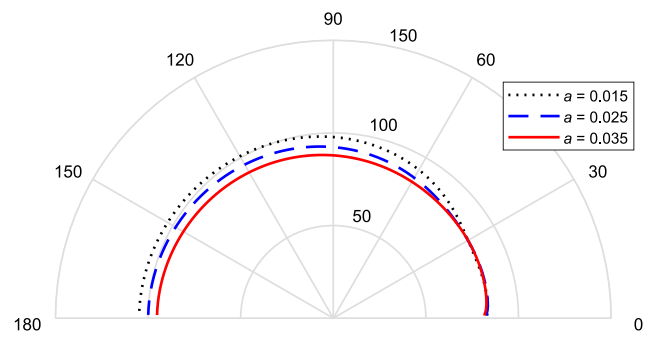

Fig. 7. Sound pressure level for different values of inner duct radius with $f = 1000$ Hz, $b = 0.050$ m, $\eta_1^{-1} = 1 - i$, $\eta_2^{-1} = 2 - i$.
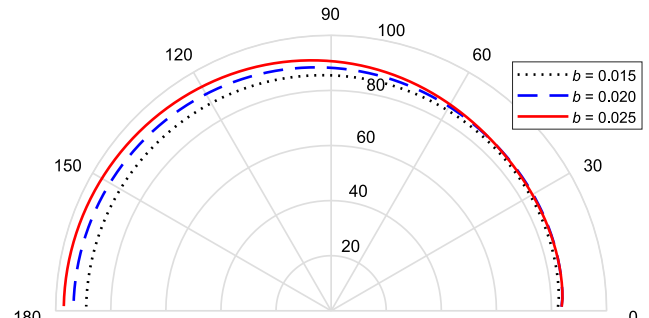

Fig. 8. Sound pressure level for different values of outer duct radius withh $f = 1000$ Hz, $a = 0.010$ m, $\eta_1^{-1} = 1 - i$, $\eta_2^{-1} = 2 - i$.
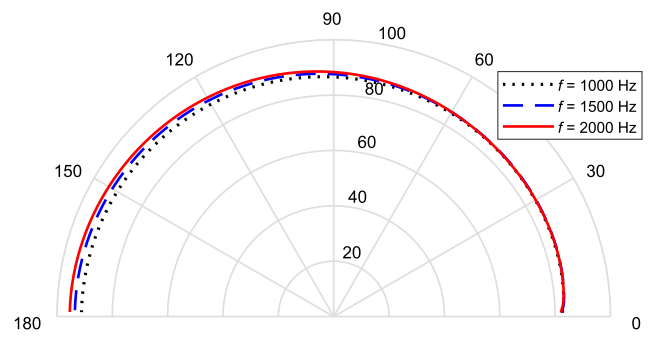

Fig. 9. Sound pressure level for different values of frequency with $a = 0.015$ m, $b = 1.5a$, $\eta_1^{-1} = 1 - i$, $\eta_2^{-1} = 2 - i$.
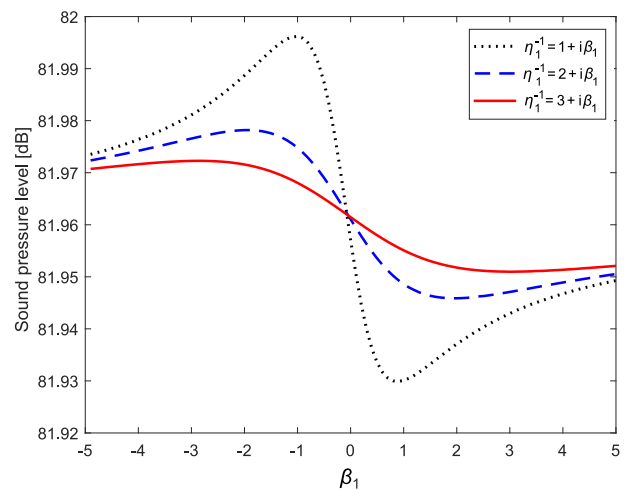

Fig. 10. Sound pressure level *versus* the imaginary part of η_1^{-1} with $f = 1000$ Hz, $a = 0.015$ m, $b = 1.5a$ m, $\eta_2^{-1} = 4 - i$.
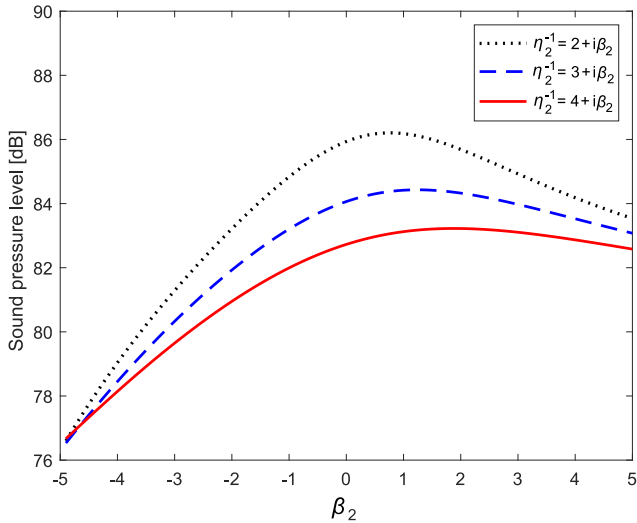
Fig. 11. Sound pressure level *versus* the imaginary part of η_2^{-1} with $f = 1000$ Hz, $a = 0.015$ m, $b = 1.5a$ m, $\eta_1^{-1} = 1 - i$.

1000 Hz. In Fig. 10, it is seen that for negative β_1 values, the sound pressure level increases as the real part of η_1^{-1} increases. However, opposite case is exist for positive β_1 values. In Fig. 11, it is observed that the sound pressure level increases rapidly as the value of β_2 increases. The effect is relatively weaker in positive values of β_2.

Figure 12 shows the variation of the sound pressure level against the frequency (f) for three different values of angle while $a = 0.025$ m, $b = 0.050$ m, $\eta_1^{-1} = 1 - i$, $\eta_2^{-1} = 2 - i$. It is observed that the sound pressure level amplitude increases with increasing values of frequency. At higher angle values this increase is more than lower ones.
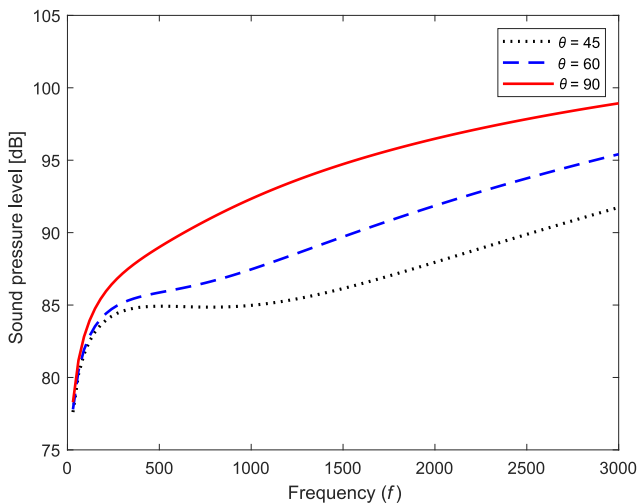

Fig. 12. Sound pressure level *versus* the frequency f with $a = 0.025$ m, $b = 0.050$ m, $\eta_1^{-1} = 1 - i$, $\eta_2^{-1} = 2 - i$.

The accuracy of the results obtained in this paper has to be investigated. Figure 13 depicts an excellent
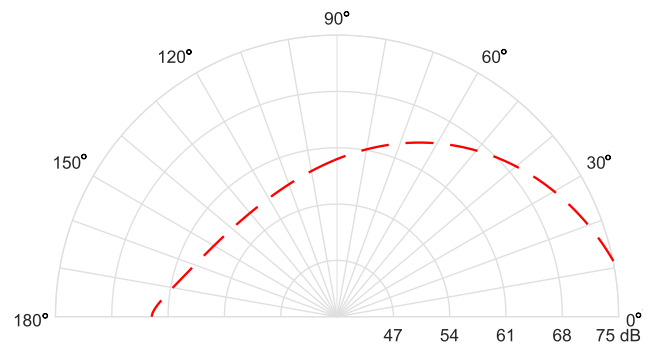

Fig. 13. Comparison of the sound pressure level with the study of (DEMIR, RIENSTRA, 2010) for rigid coaxial duct $f = 1250$ Hz.

agreement for sound pressure level between the present paper and the study of (DEMIR, RIENSTRA, 2010). When the admittances go to zero, i.e., $\eta_1, \eta_2 \to 0$, Fig. 13 is obtained for $f = 1250$ Hz. Notice that the curve corresponding to $\eta_1, \eta_2 \to 0$ coincides exactly with the result obtained in the paper by DEMIR and RIENSTRA (2010, Fig. 6a, dash line). Similar analysis is also carried out in Fig. 14 with $f = 3150$ Hz. When the admittances go to zero, the curve corresponding to $\eta_1, \eta_2 \to 0$ coincide exactly with the result obtained in (DEMIR, RIENSTRA, 2010, Fig. 8a, dash line).
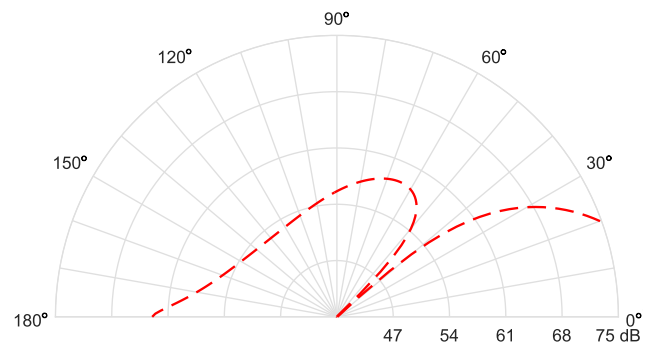

Fig. 14. Comparison of the sound pressure level with the study of (DEMIR, RIENSTRA, 2010) for rigid coaxial duct with $f = 3150$ Hz.

8. Conclusions

In this work, Wiener-Hopf technique is carried out to analyze a coaxial duct whose inner surface is lined by different acoustically absorbing materials. Some numerical results are presented to show the effects of various parameters on the sound pressure level. The results show that it is possible to obtain sound absorption by properly changing the parameters. The solution also compares well with the results where the waveguide is assumed to be rigid. Thus, in order to have further development in the noise pollution reduction, this mechanism can be included.

References

1. Buyukaksoy A., Polat B. (1998), Diffraction of acoustic waves by a semi-infinite cylindrical impedance pipe of certain wall thickness, *Journal of Engineering Mathematics*, **33**(4): 333–352, doi: 10.1023/A:1004301829276.

2. Çinar Ö.Y. (2013), Scattering of plane acoustic waves by a circular semi-infinite pipe with a rigid end face placed axially in an infinite circular duct, *Journal of Applied Mathematics and Mechanics*, **93**(12): 963–976, doi: 10.1002/zamm.201200062.

3. Çinar G., Öztürk H., Çinar Ö.Y. (2011), Reflection and transmission of plane acoustic waves in an infinite annular duct with a finite gap on the inner wall, *Mathematical Methods in Applied Sciences*, **34**(2): 220–230, doi: 10.1002/mma.1351.

4. Cremer L. (1953), Theorie der Luftschall Ddmpfung im Rechteckkanal mitschluckender Wand und das sich daboi ergebendehochste Dampfungs, *Acoustica*, **3**: 249–263.

5. Demir A., Buyukaksoy A. (2003), Radiation of plane sound waves by a rigid circular cylindrical pipe with a partial internal impedance loading, *Acta Acustica United with Acustica*, **89**(4): 578–585.

6. Demir A., Rienstra S. (2010), Sound radiation from a lined exhaust duct with lined afterbody, *16th AIAA/CEAS Aeroacoustics Conference*, 18 pages, Stockholm, Sweden, doi: 10.2514/6.2010-3947.

7. Lapin A.D. (1975), Sound attenuation in waveguides (review), *Soviet Physics Acoustics*, **21**(3): 215–222.

8. Lawrie J.B., Abrahams I.D., Linton C.M. (1993), Acoustic radiation from two opposed semi-infinite coaxial cylindrical waveguides. I: Overlapping edges, *Wave Motion*, **18**(2): 121–142, doi: 10.1016/0165-2125(93)90044-G.

9. Levine H., Schwinger J. (1948), On the radiation of sound from an unflanged circular pipe, *Physical Review*, **73**(4): 383–406, doi: 10.1103/PhysRev.73.383.

10. Morse P.M. (1939), The transmission of sound inside pipes, *Journal of the Acoustical Society of America*, **11**(2): 205–210, doi: 10.1121/1.1916024.

11. Ozturk H. (2020), Radiation of acoustic waves from a circumferential slot on a circular waveguide, *TWMS Journal of Applied and Engineering Mathematics*, **10**(3): 690–701.

12. Peake N., Abrahams I.D. (2020), Sound radiation from a semi-infinite lined duct, *Wave Motion*, **92**, 102407, doi: 10.1016/j.wavemoti.2019.102407.

13. Rawlins A.D., Jones D.S. (1978), Radiation of sound from an unflanged rigid cylindrical duct with an acoustically absorbing internal surface, *Proceedings of the Royal Society London. Series A, Mathematical and Physical Sciences*, **361**(1704): 65–91, doi: 10.1098/rspa.1978.0092.

14. Rienstra S.W. (2007), Acoustic scattering at a hard-soft lining transition in a flow duct, *Journal of Engineering Mathematics*, **59**(4): 451–475, doi: 10.1007/s10665-007-9193-z.

15. Rienstra S.W., Peake N. (2005) Modal scattering at an impedance transition in a lined flow duct, *11th AIAA/CEAS Aeroacoustics Conference*, pp. 1–19, Monterey, CA, USA, doi: 10.2514/6.2005-2852.

16. Snakowska A., Idczak H. (2006), The saddle point method applied to selected problems of acoustics, *Archives of Acoustics*, **31**(1): 57–76.

17. Snakowska A., Jurkiewicz J., Gorazd L. (2017), A hybrid method for determination of the acoustic impedanceof an unflanged cylindrical duct for multimode wave, *Journal of Sound and Vibration*, **396**: 325–339, doi: 10.1016/j.jsv.2017.02.040.

18. Tiryakioglu B. (2019), Sound radiation from the perforated end of a lined duct, *Acta Acustica united with Acustica*, **105**(4): 591–599, doi: 10.3813/ AAA.919340.

19. Tiryakioglu B. (2020), Radiation of sound waves by a semi infinite duct with outer lining and perforated end, *Archives of Acoustics*, **45**(1): 77–84, doi: 10.24425/aoa.2020.132483.

20. Tiwana M.H., Nawaz R., Mann A.B. (2017), Radiation of sound in a semi-infinite hard duct inserted axially into a larger infinite lined duct, *Analysis and Mathematical Physics*, **7**(4): 525–548, doi: 10.1007/s13324-016-0154-4.